

# Generation of Atmospheric Gravity Waves in the Polar Thermosphere in Response to Auroral Activity

S. Oyama · B.J. Watkins

Received: 29 June 2011 / Accepted: 21 October 2011 / Published online: 12 November 2011  
© Springer Science+Business Media B.V. 2011

**Abstract** Atmospheric gravity wave (AGW) is a typical phenomenon in the upper atmosphere. At mid/low latitudes, climatological sources such as unstable barometric activity in the troposphere play an important role to generate AGWs in the thermosphere. While these sources are also important at high latitudes, energy input from the magnetosphere has additional large contributions to AGW generation. This paper reviews previous studies of AGWs associated with auroral activity at high latitudes. Theoretical studies have indicated that Joule/particle heating and the Lorentz force are major processes for generating AGWs in the thermosphere. Many observations show that AGWs can propagate horizontally for thousands of km from the source region. The paper summarizes equations regarding AGW generation by Joule/particle heating and the Lorentz force, and discusses the relative importance of these two processes.

**Keywords** Atmospheric gravity wave · Aurora · High latitude · Thermosphere · Ionosphere

## 1 Introduction

Magnetic storm, ionospheric disturbance, and aurora are ionospheric signatures of disturbance in the magnetosphere. Electromagnetic and particle energy is associated with the solar wind that can directly cause such disturbances. However, some of the energy is transiently stored in the tail of magnetosphere and intermittently emitted, resulting in a magnetospheric substorm obtained mainly at high latitudes. The total energy causing individual substorms is around  $10^{15}$ – $10^{16}$  W s. Three important processes of the energy dissipation are: development of the ring current, auroral particle acceleration, and heating and plasma convection in the polar ionosphere. Approximately  $10^{11}$ – $10^{12}$  W of energy is directed to individual processes.

---

S. Oyama (✉)

Solar-Terrestrial Environment Laboratory, Nagoya University, F3-3(250), Furo Chikusa, Nagoya, Japan  
e-mail: [soyama@stelab.nagoya-u.ac.jp](mailto:soyama@stelab.nagoya-u.ac.jp)

B.J. Watkins

Geophysical Institute, University of Alaska Fairbanks, 903 Koyukuk Dr., Fairbanks, AK, 99775-7320, USA

If we assume that the heating/plasma convection energy is dissipated into the polar ionosphere at latitudes higher than  $60^\circ$ , the mean energy is of the order of  $10^{-3}$  W/m<sup>2</sup>, which is consistent with simulation results (Lu et al. 1995).

The polar ionosphere and thermosphere act as an energy and particle sink. The energy is used to heat and accelerate plasmas and neutral particles. These processes cause, for example, wind acceleration and generation of atmospheric gravity waves (AGWs) in the polar thermosphere with various spatiotemporal scales (Francis 1974; Kato et al. 1977; Hunsucker 1982; Hajkowicz 1991; Millward et al. 1993; Fujiwara et al. 1996; Fuller-Rowell et al. 1996; Hocke and Schlegel 1996; Richards and Wilkinson 1998; Smith 2000; Aruliah and Griffin 2001; Ishii et al. 2001, 2004; Oyama et al. 2001, 2008, 2010; Tsugawa et al. 2003, 2004; Aruliah et al. 2005; Nicolls and Heinselman 2007). AGWs generated in the auroral region can propagate horizontally for a long distance as detected with HF radars (Samson et al. 1990; Bristow et al. 1994) and GPS receiver networks (Ho et al. 1996, 1998; Tsugawa et al. 2003) as plasma manifestations of AGWs.

Theoretical calculations have indicated that there are at least three mechanisms in the polar thermosphere connected with the generation of AGWs: (1) perturbations in the auroral electrojet current, (2) thermospheric heating caused by highly energetic particles from the magnetosphere, and (3) rapid motions of the aurora (Chimonas and Hines 1970; Francis 1974; Brekke 1979; Williams et al. 1988; Walterscheid and Lyons 1992; Jing and Hunsucker 1993; Sun et al. 1995; Balthazor et al. 1997). The process (1) is in general more important than the process (2) (Hunsucker 1982; Hocke and Schlegel 1996). A theoretical investigation suggests that the Lorentz force tends to generate medium-scale AGWs and that Joule heating is more effective in generating large-scale AGWs (Jing and Hunsucker 1993). However, the relative contributions are not yet fully understood (Chimonas and Hines 1970; Williams et al. 1988). This paper reviews (i) effects of the Joule/particle heating and Lorentz force on AGWs' generation in the auroral thermosphere and (ii) horizontal propagation from the source.

## 2 AGW Generation

### 2.1 Particle Heating and Joule Heating

The ion production rate  $p_a$  due to auroral particle precipitation is related to the electron density by the equation (Banks 1977)

$$p_a = \alpha n_e^2 + \frac{dn_e}{dt} \quad (1)$$

where  $\alpha$  is the dissociative recombination rate at  $E$ -region altitudes, and  $n_e$  is the electron density (m<sup>-3</sup>). The time differential term can be neglect if the loss rate  $\alpha n_e^2$  is longer than the time scale of interest, which is for example a time resolution of the electron density variations. Since the profile of the rate of energy deposition from auroral electrons  $q_a$  is proportional to  $p_a$ ,  $q_a$ , also known as the particle heating rate, this can be rewritten as (Wickwar et al. 1975; Vickrey et al. 1982)

$$q_a = 5.6 \times 10^{-6} \alpha_{eff} n_e^2 \quad (2)$$

where  $\alpha_{eff} = 2.5 \times 10^{-6} \exp(-z/51.2)$  ( $z$  is height in km). The particle heating rate can temporarily exceed the Joule heating rate, particularly in an auroral arc; but on average the Joule heating rate is larger than the particle heating rate because of its extent over larger areas of the ionosphere and longer duration.

Energy transfer between the ionosphere and the thermosphere in the collisional process can be expressed by comparing the electromagnetic energy flux  $\mathbf{j} \cdot \mathbf{E}$  and the Joule heating rate  $\mathbf{j} \cdot \mathbf{E}'$  (Brekke and Rino 1978; Thayer et al. 1995; Fujii et al. 1998).

$$\mathbf{j} \cdot \mathbf{E} - \mathbf{j} \cdot \mathbf{E}' = \mathbf{u} \cdot (\mathbf{j} \times \mathbf{B}) \tag{3}$$

where  $\mathbf{j}$ ,  $\mathbf{E}$ ,  $\mathbf{u}$ , and  $\mathbf{B}$  are vectors of the current density, the electric field, the neutral wind velocity, and the magnetic field, respectively.  $\mathbf{E}' = \mathbf{E} + \mathbf{u} \times \mathbf{B}$  is the total electric field as measured in a reference frame moving with the neutral wind. Since the current density perpendicular to  $\mathbf{B}$  is given by

$$\mathbf{j}_\perp = \sigma_P \mathbf{E}' - \sigma_H \mathbf{E}' \times \mathbf{B}/B \tag{4}$$

where  $\sigma_P$  and  $\sigma_H$  are the Pedersen and Hall conductivities, respectively. The Joule heating rate  $\mathbf{j} \cdot \mathbf{E}'$  can be written as

$$\mathbf{j} \cdot \mathbf{E}' = \sigma_P (\mathbf{E} + \mathbf{u} \times \mathbf{B})^2 = \sigma_P E^2 + \sigma_P |\mathbf{u} \times \mathbf{B}|^2 - 2\sigma_P \mathbf{u} \cdot (\mathbf{E} \times \mathbf{B}) \tag{5}$$

If the neutral wind blows in the same direction as the ion velocity but with a smaller speed, the sum of the second and the third terms in the right-hand-side of (5) can be negative. In this case  $\sigma_P E^2$  is larger than the Joule heating rate (i.e.  $\mathbf{j} \cdot \mathbf{E}' < \sigma_P E^2$ ). On the other hand, if the neutral-wind speed is considerably smaller than the ion speed,  $\sigma_P E^2$  is almost equal to the Joule heating rate (i.e.  $\mathbf{j} \cdot \mathbf{E}' \approx \sigma_P E^2$ ), which is likely in the polar ionosphere.

Joule heating of the ions, which is initiated by an electric field, may be computed by applying Ohm’s law as indicated above. Subsequent increases of ion thermal energy are then transferred to the neutral gas. Since the ion density is much smaller than the neutral density, the ion temperature increases more rapidly than the neutral temperature at the onset of Joule heating. The neutral temperature increases relatively slowly compared to ion temperature increases. The neutral temperature increases then results in modulations of the pressure or the isobar. The first law of thermodynamics gives the rate of change of internal energy,  $\eta$ , as

$$\eta = \frac{dQ}{dt} - \frac{d\bar{W}}{dt} \tag{6}$$

Height-resolved data from the incoherent-scatter radar are available to calculate  $\eta$  from (2) and (5).  $dQ/dt$ , the rate of heat gained per unit volume, can be written as

$$\frac{dQ}{dt} = N_m C_p \frac{dT}{dt} = N_m C_p \frac{dT}{dl} \frac{dl}{dt} = N_m C_p \frac{dT}{dl} u_l \tag{7}$$

where  $N_m$  is the mass density of neutrals,  $C_p$  is the specific heat at constant pressure,  $T$  is the temperature of neutrals, and  $u_l$  is the wind flowing on the isobar in a direction  $l$ .

$$\frac{d\bar{W}}{dt} = \frac{dP}{dt} = \frac{dP}{dl} \frac{dl}{dt} = \frac{dP}{dl} u_l \tag{8}$$

is the rate at which work is done per unit volume, and  $P$  is the pressure. Substituting (7) and (8) into (6) gives  $u_l$  as

$$u_l = \frac{\eta}{N_m (C_p - k / (\langle m \rangle m_p)) dT/dl} \tag{9}$$

assuming  $P = (N_m k T) / (\langle m \rangle m_p)$ , where  $\langle m \rangle$  and  $m_p$  are the mean neutral mass and the proton mass, respectively, and  $k$  is the Boltzmann constant. The gradient of  $N_m$  along  $l$  is assumed to be zero ( $dN_m/dl = 0$ ). For example, horizontal winds of 100–300 m/s may be generated in the  $E$  region in association with the temperature gradient of  $\sim 2 \times 10^{-4}$  K/m (Oyama et al. 2008).

Equation (9) represents wind along the isobar or  $l$  in association with natural ionospheric/thermospheric heating. Precisely speaking the pressure  $P$  also has some gradients in the direction perpendicular to  $l$ . However, the wind flux across the isobar is considered to be much smaller than the  $l$  component. Since  $l$  is almost parallel to the earth surface,  $u_l$  can be regarded as the geographically horizontal component of the wind. The horizontal wind acceleration contributes to equatorward propagation of AGW and TID (traveling ionospheric disturbance) from auroral latitudes (Fujiwara et al. 1996).

An assumption of no vertical wind is not always appropriate, for example in the vicinity of an auroral arc. The geographically vertical component of the wind flowing along the isobar may be comparable to the horizontal component (Oyama et al. 2008; Kurihara et al. 2009). To a reasonable approximation, the atmosphere is balanced in equilibrium between gravity and the vertical pressure gradient. Vertical displacement of an air parcel tends to be compensated by the pressure, temporarily destroying the balance with gravity; then, if no other force comes into play, the air parcel seeks to return to equilibrium by oscillating at a certain unique frequency, which is called the Brunt-Väisälä or buoyancy frequency. This frequency is a function of temperature, decreasing with height in the thermosphere:  $3 \times 10^{-2}$  and  $1 \times 10^{-2}$  Hz (corresponding to  $\sim 4$  and  $\sim 10$  minutes, respectively) at  $\sim 120$  km and  $\sim 200$  km height, respectively (Walterscheid et al. 2001). According to the dispersion relation proposed by Hines (1960), AGW frequency should be lower than the Brunt-Väisälä frequency. While the quantitative understanding of the generation mechanism is not well developed, there is experimental evidence to show thermospheric wind perturbations near the discrete auroral arc (Oyama et al. 2008, and references therein). If one calculates a spectrum from temporal and/or spatial data taken near the source region, the spectrum should not have specific peaks. However, some of the wave packets may grow to a monochromatic wave observed as an AGW propagating horizontally from the source region.

### 2.2 Ion Drag and Relative Importance to Joule Heating

The fundamental mechanism of the Joule heating process is collisions between ions and neutral particles initiated by an electric field. For ion drag, the collision process is also essential. Collisions result in increase of thermal and kinetic energy for Joule heating and ion drag, respectively. To be more specific regarding neutral particle motion, plasma energy is used to increase random velocity (as thermal motion) and flow velocity (as bulk motion with an average direction) for Joule heating and ion drag, respectively.

The Lorentz force can be written as

$$\mathbf{f}_L = \frac{\mathbf{j} \times \mathbf{B}}{\rho} \tag{10}$$

where  $\rho$  is the neutral mass density. While both the Lorentz force and Joule heating come into play to generate AGWs in the polar thermosphere, the relative importance (denoted as  $L/J$  in this paper) is not simply derived as the ratio of  $\mathbf{f}_L$  to  $\mathbf{j} \cdot \mathbf{E}'$  because we should take into account the ion-neutral collision frequency in a more precise manner. In the work by Chimonas and Hines (1970)  $L/J$  is expressed as

$$\frac{L}{J} = \frac{gHB}{C_L} \frac{\sigma_c}{j} \tag{11}$$

where  $\sigma_c$  and  $j$  are the Cowling conductivity and current density, respectively, and  $C_L$  is the phase speed of AGW. Brekke (1979) derives dependency of  $L/J$  on ion-neutral collision frequency  $\nu_{in}$  and ion gyrofrequency  $\Omega_i$  as shown in (12).

$$\frac{L}{J} \approx 15 \sqrt{\frac{\Omega_i^2 + \nu_{in}^2}{\Omega_i^2}} \frac{1}{E} \tag{12}$$

Since  $\sqrt{(\Omega_i^2 + v_{in}^2)/\Omega_i^2}$  decreases with height, the relative importance  $L/J$  also decreases with height. This means that the contribution of Joule heating becomes larger with height. However, many observation and simulation studies suggest that the ion drag can modulate the horizontal wind pattern at polar  $F$ -region heights although the response is relatively sluggish at  $E$ -region heights (Conde and Smith 1998, and references therein). To clarify this issue, a consideration of the temperature dependence on  $L/J$  is helpful, although our understanding is not yet fully developed.

Richmond (1978) calculates individual contributions of the Lorentz force and Joule heating for generating AGWs:

$$L = \frac{\sigma_P B}{\rho} E_x u_y, \tag{13}$$

and

$$J = \frac{\sigma_P}{\rho} E_x^2 \frac{H'}{H\zeta}, \tag{14}$$

where  $E_x$  and  $u_y$  are one of the horizontal components of electric field and neutral wind velocity, respectively,  $H'$  is perturbation of the scale height  $H$ , and  $\zeta$  is dimensionless parameter representing static stability. For simplicity one of the horizontal components is considered for the Lorentz force contribution. The relative importance  $L/J$  can be estimated in the first approximation form as

$$\frac{L}{J} = \frac{Bu_y}{E_x} \bigg/ \frac{H'}{H\zeta} \propto \frac{Bu_y}{E_x} \bigg/ \frac{T'}{T} \tag{15}$$

$E_x$  is not equivalent to  $Bu_y$  in the lower thermosphere (below  $\sim 120$  km) because of collisions between ions and neutral particles. There is a tendency for the wind velocity to be correlated with the Lorentz force and for the temperature perturbation to be correlated with Joule heating. Thus both terms come into play for generating AGWs in the lower thermosphere. However, in the upper thermosphere (corresponding to  $F$ -region heights), (15) may be more simplified as  $L/J \propto T/T'$  because the horizontal neutral wind is more effectively accelerated along the ion velocity by the ion drag, that is, acceptable for assumption that  $Bu_y$  more quickly follows  $E_x$  variations. The neutral temperature can be perturbed by Joule heating but not by the Lorentz force. Therefore it is considered that Joule heating becomes more important for AGW generation in the upper thermosphere than the Lorentz force. The theoretical prediction of  $L/J$  made of data from the Chatanika incoherent-scatter radar was 0.1–10 for periods of moderately geomagnetic disturbance, and the average value of  $L/J$  was 2.37 for a mean electric-field magnitude of  $\sim 43$  mV/m (Hunsucker 1982). The theoretical calculation by Brekke (1979) showed that the value of  $L/J$  at 140 km height was smaller than that at 100 km height by about two orders.

If we can estimate  $T'/T$  from measurements, one might think that  $T'/T$  increases with height because (12) suggests that  $L/J$  decreases with height. It is generally difficult to obtain the height-resolved neutral temperature from measurements; therefore ion temperature perturbations measured with incoherent-scatter radar have been studied as a tracer (Shibata and Schlegel 1993; Kirchengast et al. 1996). The results show that  $T'_i/T_i$  ( $T_i$ : ion temperature) decreases with height in the upper ionosphere. This trend is the opposite sense of the theoretical prediction by (12). However,  $T'_i/T_i$  increases with height for the case of lower-period band (14–60 minutes) in the lower thermosphere (Shibata and Schlegel 1993), which is consistent with (12).

### 3 AGW/TID Propagation

Energy input from the magnetosphere into the polar ionosphere/thermosphere has various temporal and spatial evolutions in the vicinity of the auroral arc much like complex arc structures. While the thermosphere results in temperature increases and wind acceleration from the energy input, the time constant of the thermospheric change depends on the energy transfer process. Furthermore, inertia, which plays an important role in the thermospheric wind dynamics below  $\sim 200$  km (Lindzen 1967), delays the thermospheric response. It is

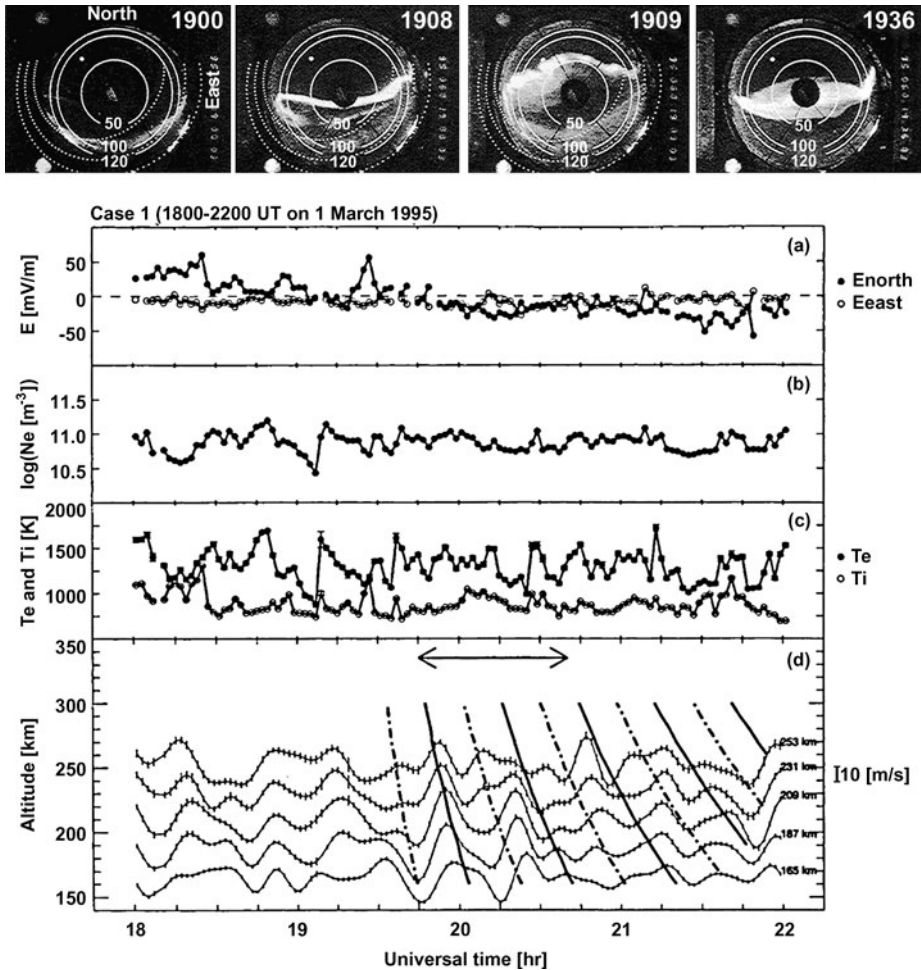
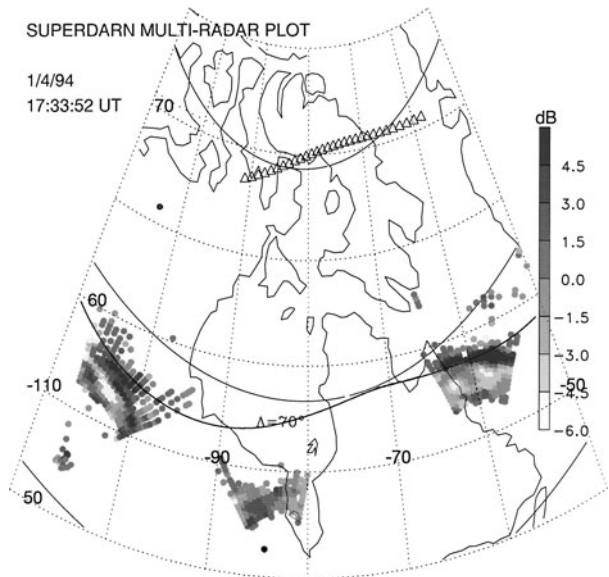


**Fig. 1** Top panel shows all-sky camera images taken at Kilpisjärvi, Finland at 19:00, 19:08, 19:09, and 19:36 UT on 1 March 1995. The three circles shown with solid lines indicate distances of 50, 100, and 120 km from the zenith at Kilpisjärvi. The dotted curves indicate distances of 140, 200, and 290 km from the magnetic field line at Tromsø, Norway at an altitude of 110 km. Four panels below present temporal variations of the EISCAT Tromsø UHF radar data of (a) electric field, (b) electron density at 209 km, (c) electron and ion temperatures at 209 km, and (d) field-aligned component of the neutral wind velocity from 165 to 253 km altitudes. The modeled phase lines with minimum and maximum values are plotted with thick dash-dotted and thick solid lines, respectively. This study concluded that observed oscillations in the field-aligned neutral wind velocity was generated by poleward expansion of the auroral arc (after Oyama et al. 2001)

**Fig. 2** A backscatter-echo map of SuperDARN radar data from 17:33 UT on January 4, 1994, showing the location of a gravity wave phase front and the estimated source region (marked by triangles) (after Bristow and Greenwald 1996)



thus generally difficult to find a source of the observed AGWs. However, some studies succeeded in identifying the source region of AGWs. Oyama et al. (2001) reported that AGWs at  $F$ -region heights were measured with the incoherent-scatter radar coincident with poleward expansion of the auroral arc (see Fig. 1). They estimated the horizontal phase speed, and compared with the distance to the arc measured with an all-sky camera in order to determine the source region. The horizontal wavelength of AGWs was comparable with the distance to the source (about 200 km) in their study. Thus in this case the waves propagated for only one wavelength until detected by the radar.

It is known that auroral AGWs can propagate horizontally for great distances. To detect them we need multiple instruments spaced horizontally or an instrument capable of observing over a wide area. The former examples are total electron content maps derived with GPS receiver networks (Tsugawa et al. 2003, 2004) and ionosonde networks (Maeda and Handa 1980; Hajkowicz and Hunsucker 1987; Hajkowicz 1990, 1991, 1999), and the latter example is an HF radar (Bristow et al. 1994, 1996; Bristow and Greenwald 1996). A case study of LSTIDs (large scale TIDs) measured with ionosondes in both hemispheres shows equatorward propagation of the wave, and its source region has been located along an  $L$ -shell with  $L$ -value of 4–5 (Hajkowicz and Hunsucker 1987). Statistics of TEC data in Japan for 45 months show that the occurrence rate of equatorward propagating LSTIDs increases with  $Kp$  index (Tsugawa et al. 2004). A horizontal map of the ground-backscatter power of the HF radar can be used to find the wave front (Bristow and Greenwald 1996) (see Fig. 2). Bristow et al. (1994) calculate propagation direction, speed, horizontal wavelength, and oscillation period from the HF radar data, and suggest that multiple waves from multiple directions are a common feature of the observations. While results of ionosonde and TEC present equatorward propagation of TIDs during periods of geomagnetic disturbance, statistics of the HF radar data suggest that TIDs can also propagate poleward from the auroral oval although there has been no observation of this yet.

Another important issue that requires more research is the damping rate, which is related to the energy dissipation rate. Tsugawa et al. (2003) calculated spatial variations of the LSTIDs' amplitude ratio along the propagation direction (see Fig 3). The  $e$ -folding distance

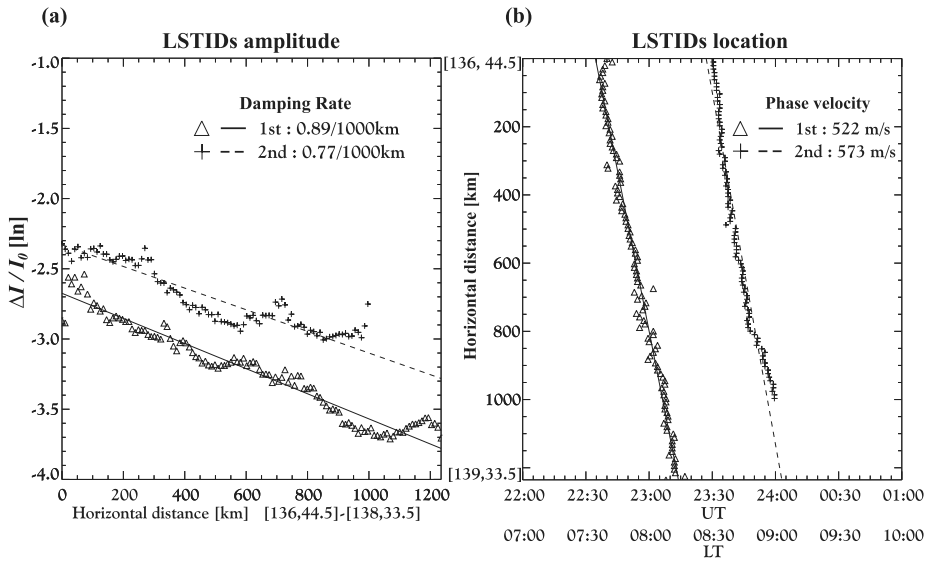


**Fig. 3** Spatial variations of (a) the AGW-amplitude maxima and (b) temporal variations of their locations for the two LSTIDs. These maximum values and least-square fitted lines are represented by *open triangles* and a *solid line* for the first LSTID, and *crosses* and a *broken line* for the second LSTID, respectively (after Tsugawa et al. 2003)

was 961 km in the afternoon sector but smaller in the night sector. They concluded that the ion drag played an important role in damping LSTIDs.

#### 4 Summary and Outstanding Questions

Atmospheric gravity wave at high latitudes is one of the thermospheric responses to the energy input from the magnetosphere. Joule heating, auroral particle heating, and ion drag play important roles in generating AGWs. However, debate remains about how much energy the thermosphere needs to generate AGWs, especially in the lower thermosphere (90–150 km heights). Previous results of numerical simulations provide strong evidence that it is difficult to reproduce wind and temperature fluctuations that simulate experimental values (observed with Fabry-Perot interferometer, incoherent-scatter radar, etc.) in the lower thermosphere unless the heating rate used in the model code is considerably larger and/or the heating duration is longer than a typical measured values (Sun et al. 1995; Shinagawa and Oyama 2006). Propagation distance of the AGW/TID from the source is also a question that remains to be answered. Since it may be difficult to identify the start/end point of a wave packet, the damping rate is more helpful for estimating the propagation distance. The damping rate is a key parameter for understanding the momentum dissipation process during wave propagation from high to mid/low latitudes.

Atmospheric gravity waves can be seen in the thermosphere even during geomagnetically quiet periods. Figure 4 shows a height-time profile of the field-aligned ion velocity measured with the European Incoherent Scatter (EISCAT) Svalbard radar. Periodic variations (at oscillation period of  $\sim 1$  hour) are clearly seen from 00 to 04 UT on 14 August 2007 with changing sign. This is a very clear example of the AGW/TID in the thermosphere/ionosphere.



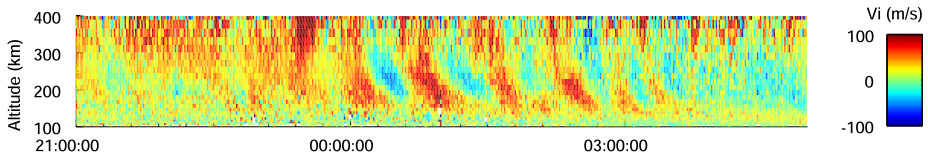


**Fig. 4** Height-time profile of the field-aligned ion velocity measured with the EISCAT Svalbard radar from 21 UT on 13 August to 05 UT on 14 August 2007. Positive is upward along the magnetic field line. Wave patterns are clearly seen from 00 to 04 UT

Since magnetometer data suggest that the geomagnetic activity was quiet for this interval (not shown here), it is considered that the wave structure must have been generated independent of electromagnetic energy. The generation mechanism of this example is not clear but the effect of the lower atmosphere is an important issue to be understood separate from auroral effects.

**Acknowledgements** This research has been supported by a Grant-in-Aid for Scientific Research (2240-3010) from MEXT, Japan. We are indebted to the director and staff of EISCAT for operating the facility and supplying the data. EISCAT is an international association supported by research organizations in China (CRIPR), Finland (SA), Germany (DFG), Japan (STEL and NIPR), Norway (NFR), Sweden (VR), and the United Kingdom (STFC).

## References

- A.L. Aruliah, E.M. Griffin, Evidence of meso-scale structure in the high-latitude thermosphere. *Ann. Geophys.* **19**, 36–46 (2001)
- A.L. Aruliah, E.M. Griffin, A.D. Aylward, E.A.K. Ford, M.J. Kosch, C.J. Davis, V.S.C. Howells, S.E. Pryse, H.R. Middleton, J. Jussila, First direct evidence of meso-scale variability on ion-neutral dynamics using co-located tristatic FPIs and EISCAT radar in Northern Scandinavia. *Ann. Geophys.* **23**, 147–162 (2005)
- R.L. Balthazor, R.J. Moffett, G.H. Millward, A study of the Joule and Lorentz inputs in the production of atmospheric gravity waves in the upper thermosphere. *Ann. Geophys.* **15**, 779–785 (1997)
- P.M. Banks, Observations of Joule and particle heating in the auroral zone. *J. Atmos. Terr. Phys.* **39**, 179–193 (1977)
- A. Brekke, On the relative importance of Joule heating and the Lorentz force in generating atmospheric gravity waves and infrasound waves in the auroral electrojets. *J. Atmos. Terr. Phys.* **41**, 475–479 (1979)
- A. Brekke, C.L. Rino, High-resolution altitude profiles of the auroral zone energy dissipation due to ionospheric currents. *J. Geophys. Res.* **83**(A6), 2517–2524 (1978)
- W.A. Bristow, R.A. Greenwald, Multiradar observations of medium-scale acoustic gravity waves using the Super Dual Auroral Radar Network. *J. Geophys. Res.* **101**(A11), 24,499–24,511 (1996)
- W.A. Bristow, R.A. Greenwald, J.C. Samson, Identification of high-latitude acoustic gravity wave sources using the Goose Bay HF radar. *J. Geophys. Res.* **99**(A1), 319–331 (1994)
- W.A. Bristow, R.A. Greenwald, J.P. Villain, On the seasonal dependence of medium-scale atmospheric gravity waves in the upper atmosphere at high latitudes. *J. Geophys. Res.* **101**(A7), 15,685–15,699 (1996)
- G. Chimonas, C.O. Hines, Atmospheric gravity waves launched by auroral currents. *Planet. Space Sci.* **18**, 565–582 (1970)
- M. Conde, R.W. Smith, Spatial structure in the thermospheric horizontal wind above Poker Flat, Alaska, during solar minimum. *J. Geophys. Res.* **103**(A5), 9449–9471 (1998)
- S.H. Francis, A theory of medium-scale travelling ionospheric disturbances. *J. Geophys. Res.* **79**, 5245–5260 (1974)
- R. Fujii, S. Nozawa, N. Matuura, A. Brekke, Study on neutral wind contribution to the electrodynamics in the polar ionosphere using EISCAT CP-1 data. *J. Geophys. Res.* **103**(A7), 14,731–14,739 (1998)
- H. Fujiwara, S. Maeda, H. Fukunishi, T.J. Fuller-Rowell, D.S. Evans, Global variations of thermospheric winds and temperatures caused by substorm energy injection. *J. Geophys. Res.* **101**, 225–239 (1996)
- T.J. Fuller-Rowell, M.V. Codrescu, H. Rishbeth, R.J. Moffett, S. Quegan, On the seasonal response of the thermosphere and ionosphere to geomagnetic storms. *J. Geophys. Res.* **101**(A2), 2343–2353 (1996)

- L.A. Hajkowicz, A global study of large scale travelling ionospheric disturbances (TIDs) following a step-like onset of auroral substorms in both hemispheres. *Planet. Space Sci.* **38**, 913–923 (1990)
- L.A. Hajkowicz, Auroral electrojet effect on the global occurrence pattern of large scale travelling ionospheric disturbances. *Planet. Space Sci.* **39**, 1189–1196 (1991)
- L.A. Hajkowicz, Monitoring ionospheric response to auroral electrojet activity from sub-auroral to equatorial latitudes in the East Asian-Australian longitudinal sector over a solar cycle (1978–1986). *J. Atmos. Sol.-Terr. Phys.* **61**, 857–866 (1999)
- L.A. Hajkowicz, R.D. Hunsucker, A simultaneous observation of large-scale periodic TIDs in both hemispheres following an onset of auroral disturbances. *Planet. Space Sci.* **35**, 785–791 (1987)
- C.O. Hines, Internal atmospheric gravity waves at ionospheric heights. *Can. J. Phys.* **38**, 1441–1481 (1960)
- C.M. Ho, A.J. Mannucci, U.J. Lindqwister, X. Pi, B.T. Tsurutani, Global ionosphere perturbations monitored by the Worldwide GPS Network. *Geophys. Res. Lett.* **23**(22), 3219–3222 (1996)
- C.M. Ho, A.J. Mannucci, L. Sparks, X. Pi, U.J. Lindqwister, B.D. Wilson, B.A. Iijima, M.J. Reyes, Ionospheric total electron content perturbations monitored by the GPS global network during two northern hemisphere winter storms. *J. Geophys. Res.* **103**(A11), 26,409–26,420 (1998)
- K. Hocke, K. Schlegel, A review of atmospheric gravity waves and travelling ionospheric disturbances: 1982–1995. *Ann. Geophys.* **14**, 917–940 (1996)
- R.D. Hunsucker, Atmospheric gravity waves generated in the high-latitude ionosphere: a review. *Rev. Geophys.* **20**, 293–315 (1982)
- M. Ishii, M. Conde, R.W. Smith, M. Krynicki, E. Sagawa, S. Watari, Vertical wind observations with two Fabry-Perot interferometers at Poker Flat, Alaska. *J. Geophys. Res.* **106**, 10,537–10,551 (2001)
- M. Ishii, M. Kubota, M. Conde, R.W. Smith, M. Krynicki, Vertical wind distribution in the polar thermosphere during Horizontal *E* Region Experiment (HEX) campaign. *J. Geophys. Res.* **109**, A12311 (2004). doi:[10.1029/2004JA010657](https://doi.org/10.1029/2004JA010657)
- J. Jing, R.D. Hunsucker, A theoretical investigation of sources of large and medium scale atmospheric gravity waves in the auroral oval. *J. Atmos. Terr. Phys.* **55**, 1667–1679 (1993)
- S. Kato, T. Kawakami, D. St. John, Theory of gravity wave emission from moving sources in the upper atmosphere. *J. Atmos. Terr. Phys.* **39**, 581–588 (1977)
- G. Kirchengast, K. Hocke, K. Schlegel, The gravity wave-TID relationship: insight via theoretical model-EISCAT data comparison. *J. Atmos. Terr. Phys.* **58**(1–4), 233–243 (1996)
- J. Kurihara, S. Oyama, S. Nozawa, T.T. Tsuda, R. Fujii, Y. Ogawa, H. Miyaoka, N. Iwagami, T. Abe, K.-I. Oyama, M.J. Kosch, A. Aruliah, E. Griffin, K. Kauristie, Temperature enhancements and vertical winds in the lower thermosphere associated with auroral heating during the DELTA campaign. *J. Geophys. Res.* **114**, A12306 (2009). doi:[10.1029/2009JA014392](https://doi.org/10.1029/2009JA014392)
- R.S. Lindzen, Reconsideration of diurnal velocity oscillation in the thermosphere. *J. Geophys. Res.* **72**(5), 1591–1598 (1967)
- G. Lu, A.D. Richmond, B.A. Emery, R.G. Roble, Magnetosphere-ionosphere-thermosphere coupling: effect of neutral winds on energy transfer and field-aligned current. *J. Geophys. Res.* **100**(A10), 19,643–19,659 (1995)
- S. Maeda, S. Handa, Transmission of large-scale TIDs in the ionospheric F2-region. *J. Atmos. Terr. Phys.* **42**, 853–859 (1980)
- G.H. Millward, S. Quegan, R.J. Moffett, T.J. Fuller-Rowell, D. Rees, A modeling study of the coupled ionospheric and thermospheric response to an enhanced high-latitude electric field event. *Planet. Space Sci.* **41**, 45–56 (1993)
- M.J. Nicolls, C.J. Heinselman, Three-dimensional measurements of travelling ionospheric disturbances with the Poker Flat incoherent scatter radar. *Geophys. Res. Lett.* **34**, L21104 (2007). doi:[10.1029/2007GL031506](https://doi.org/10.1029/2007GL031506)
- S. Oyama, M. Ishii, Y. Murayama, H. Shinagawa, S.C. Buchert, R. Fujii, W. Kofman, Generation of atmospheric gravity waves associated with auroral activity in the polar *F* region. *J. Geophys. Res.* **106**(A9), 18,543–18,554 (2001)
- S. Oyama, K. Shiokawa, J. Kurihara, T.T. Tsuda, S. Nozawa, Y. Ogawa, Y. Otsuka, B.J. Watkins, Lower-thermospheric wind fluctuations measured with an FPI during pulsating aurora at Tromsø, Norway. *Ann. Geophys.* **28**, 1847–1857 (2010)
- S. Oyama, B.J. Watkins, S. Maeda, H. Shinagawa, S. Nozawa, Y. Ogawa, A. Brekke, C. Lathuillere, W. Kofman, Generation of the lower-thermospheric vertical wind estimated with the EISCAT KST radar at high latitudes during periods of moderate geomagnetic disturbance. *Ann. Geophys.* **26**, 1491–1505 (2008)
- P.G. Richards, P.J. Wilkinson, The ionosphere and thermosphere at southern midlatitudes during the November 1993 ionospheric storm: a comparison of measurement and modeling. *J. Geophys. Res.* **103**(A5), 9373–9389 (1998)
- A. Richmond, Gravity wave generation, propagation, and dissipation in the thermosphere. *J. Geophys. Res.* **83**(A9), 4131–4145 (1978)

- J.C. Samson, R.A. Greenwald, J.M. Ruohoniemi, A. Frey, K.B. Baker, Goose Bay radar observations of earth-reflected, atmospheric gravity waves in the high-latitude ionosphere. *J. Geophys. Res.* **95**(A6), 7693–7709 (1990)
- T. Shibata, K. Schlegel, Vertical structure of AGW associated ionospheric fluctuations in the E- and lower F-region observed with EISCAT—a case study. *J. Atmos. Terr. Phys.* **55**(4/5), 739–749 (1993)
- H. Shinagawa, S. Oyama, A two-dimensional simulation of thermospheric vertical winds in the vicinity of an auroral arc. *Earth Planets Space* **58**, 1173–1181 (2006)
- R.W. Smith, The global-scale effect of small-scale thermospheric disturbances. *J. Atmos. Sol.-Terr. Phys.* **62**, 1623–1628 (2000)
- Z.P. Sun, R.P. Turco, R.L. Walterscheid, S.V. Venkateswaran, P.W. Jones, Thermospheric response to morningside diffuse aurora: high-resolution three-dimensional simulations. *J. Geophys. Res.* **100**, 23,779–23,793 (1995)
- J.P. Thayer, J.F. Vickrey, R.A. Heelis, J.B. Gary, Interpretation and modeling of the high-latitude electromagnetic energy flux. *J. Geophys. Res.* **100**(A10), 19,715–19,728 (1995)
- T. Tsugawa, A. Saito, Y. Otsuka, A statistical study of large-scale traveling ionospheric disturbances using the GPS network in Japan. *J. Geophys. Res.* **109**, A06302 (2004). doi:[10.1029/2003JA010302](https://doi.org/10.1029/2003JA010302)
- T. Tsugawa, A. Saito, Y. Otsuka, M. Yamamoto, Damping of large-scale traveling ionospheric disturbances detected with GPS networks during the geomagnetic storm. *J. Geophys. Res.* **108**(A3), 1127 (2003). doi:[10.1029/2002JA009433](https://doi.org/10.1029/2002JA009433)
- J. Vickrey, R. Vondrak, S. Matthews, Energy deposition by precipitating particles and Joule dissipation in the auroral ionosphere. *J. Geophys. Res.* **87**(A7), 5184–5196 (1982)
- R.L. Walterscheid, L.R. Lyons, The neutral circulation in the vicinity of a stable auroral arc. *J. Geophys. Res.* **97**, A12 (1992). doi:[10.1029/92JA01730](https://doi.org/10.1029/92JA01730)
- R. Walterscheid, G. Schubert, D. Brinkman, Small-scale gravity waves in the upper mesosphere and lower thermosphere generated by deep tropical convection. *J. Geophys. Res.* **106**(D23), 31825–31832 (2001)
- V.B. Wickwar, M.J. Baron, R.D. Sears, Auroral energy input from energetic electrons and Joule heating at Chatanika. *J. Geophys. Eng.* **80**(31), 4364–4367 (1975)
- P.J.S. Williams, G. Crowley, K. Schlegel, T.S. Virdi, I. McCrea, G. Watkins, N. Wade, J.K. Hargreaves, T. Lachlan-Cope, H. Muller, J.E. Baldwin, P. Warner, A.P. van Eyken, M.A. Hapgood, A.S. Rodger, The generation and propagation of atmospheric gravity waves observed during the Worldwide Atmospheric Gravity-wave Study (WAGS). *J. Atmos. Terr. Phys.* **50**(4/5), 323–338 (1988)